Kinetic and thermodynamic studies on the cyanation reactions and base-on/base-off equilibria of alkyl-13-epicobalamins †

Mohamed S. A. Hamza,[a,b] Xiang Zou,[c] Kenneth L. Brown[c] and Rudi van Eldik *[a]

[a] *Institute for Inorganic Chemistry, University of Erlangen-Nürnberg, Egerlandstr.1, 91058 Erlangen, Germany. E-mail: vaneldik@chimie.uni-erlangen.de*
[b] *Department of Chemistry, Faculty of Science, Ain Shams University, Cairo, Egypt*
[c] *Department of Chemistry and Biochemistry, Ohio University, Athens, Ohio 45701, USA*

Ligand substitution equilibria of two different 13-epicobalamins (X-13-epiCbl, X = NCCH$_2$ and CN$^-$) with cyanide have been studied. It was found that CN$^-$ substitutes the 5,6-dimethylbenzimidazole (DMBz) moiety in the α-position to form X(CN)Cbl-13epi, which for X = NCCH$_2$ in the presence of CN$^-$ subsequently gives (CN)$_2$Cbl-13epi. The kinetics of the displacement of DMBz by CN$^-$ showed saturation behaviour at high cyanide concentration and the limiting rate constants are characterized by the activation parameters: X = NCCH$_2$, $\Delta H^{\neq}$ = 83 ± 1 kJ mol^{-1}, $\Delta S^{\neq}$ = +77 ± 4 J K^{-1} mol^{-1}, $\Delta V^{\neq}$ = +13.3 ± 1.0 cm^3 mol^{-1}; X = CN$^-$, $\Delta H^{\neq}$ = 106 ± 1 kJ mol^{-1}, $\Delta S^{\neq}$ = +82 ± 4 J K^{-1} mol^{-1} and $\Delta V^{\neq}$ = +14.8 ± 0.5 cm^3 mol^{-1}. These parameters are interpreted in terms of a limiting D mechanism. The rate constants for the displacement of DMBz in the case of the 13-epicobalamins were found to be slower than those obtained in the case of the analogous alkylcobalamins, and consequently, the thermodynamic equilibrium constants for the 13-epicobalamins were found to be smaller than those obtained in the case of the alkylcobalmins. This clearly shows the effect of the epimerization of the *e*-side chain attached to the C-13 of the corrin ring on the rate and equilibrium constants for these ligand displacement reactions.

Introduction

There is significant interest in studying the axial ligand substitution reactions of cobalt–corrinoid complexes since it is known that the two active cobalamins (methylcobalamin, MeCbl, and coenzyme B$_{12}$, AdoCbl) undergo substitution of their axial benzimidazole ligand by a protein histidine residue during complexation to the CH$_3$Cbl-dependent methionine synthase,[1,2] the class I[3] AdoCbl-dependent mutases (methyl-malonyl-coenzyme A mutase and glutamate mutase),[4,5] and the class III AdoCbl-dependent D-lysine-5,6-aminomutase.[6] As a result, comparison of the ligand substitution reactions *trans* to the axial alkyl ligand in coenzyme B$_{12}$ and its derivatives to that *trans* to a non-alkyl ligand is of interest to further our understanding of the mechanisms of these reactions.

The corrin ring (macrocyclic tetrapyrrole ring) does not possess a plane of symmetry, and consequently, there is a possibility of axial ligand diastereomerism when the two axial ligands are different.[7–13] The "upper", or β-face, of the corrinoid, with its upward projecting *a, c* and *g* acetamide side chain, is less sterically hindered than the "lower", or α-face, which is bracketed by the downward projecting *b, d* and *e* propionamides and the secondary amide *f* side chain. The electronic structure of the corrin ring has a significant effect on the properties of the Co(III) ion. It has been shown recently that displacement of H at C10 by an electron-withdrawing NO group increases the pK_a for coordinated H$_2$O, renders the Co–O bond more ionic and significantly deactivates the metal ion towards ligand substitution.[14]

It is known that many structurally modified analogs of AdoCbl, including those modified in the side chains,[15] in the corrin ring itself,[16] in the nucleotide loop[15a,17] and in the adenine moiety itself,[18] are active coenzymes with some AdoCbl-dependent enzymes. These active analogs are very important in understanding the mechanism by which the B$_{12}$-requiring enzymes activate AdoCbl. An interesting example of these active coenzyme analogs is the C13 epimer,[19,20] in which the *e* propionamide side chain adopts an "upwardly" axial configur-

ation. X-Ray crystal structures of CN-13-epiCbl[21,22] and molecular mechanics calculations[23] showed that epimerization at C13 leads to twisting of the C pyrrol ring and an "upwardly" axial disposition of the *e* side chain. Epimerization at C13 causes a decrease in p$K_{\text{base-off}}$ of about 0.83 ± 0.14 across the series of XCbl and a corresponding increase in K_{Co}, for a given X. K_{Co} was found to be 6.9 ± 1.8 fold higher for the X-13-epiCbl's than for the XCbl's.[24]

We have been interested in the application of different kinetic and thermodynamic high pressure techniques to study the ligand substitution reactions of a series of alkylcobalamins (XCbl) in efforts to understand the mechanism of these reactions and to investigate how the alkyl group (X) in the trans position controls the kinetics and thermodynamics of these reactions. In this work, the fascinating influence of a single cobalt–carbon bond in tuning the reactivity of the Co(III) center was clearly demonstrated.[25–29] We found that the reaction of XCbl with CN$^-$, where X = NCCH$_2$, CF$_3$ and CN$^-$, proceeded via the formation of an intermediate X(CN)Cbl, which subsequently reacts, in the presence of CN$^-$, to give (CN)$_2$Cbl$^-$.[26] We also found that the mechanism of substituting the axial DMBz *trans* to the X group in a series of XCbl by CN$^-$ occurred via a dissociative mechanism.[25,26]

In order to further improve our understanding of the reaction mechanism of such cobalamins and their derivatives, we have now investigated the effect of epimerization at C13 on the kinetics and thermodynamics of ligand substitution reactions of these complexes. We have studied the cyanation reactions of two alkyl-13-epicobalamins, in which the alkyl group was NCCH$_2$ and CN$^-$. For this purpose the kinetics of the substitution reactions with cyanide was studied as a function of nucleophile concentration, temperature and pressure.

Experimental

Materials

All chemicals were of analytical grade and used as received. CAPS buffer was purchased from Sigma. HClO$_4$, NaClO$_4$ and NaCN were purchased from Merck. Ultra pure water was used in the kinetic and thermodynamic measurements. The sample preparations and all measurements were carried out in

diffuse light since alkyl-13-epicobalamins, like all other alkyl-cobalamins, are known to be very light sensitive.[30]

Cyanocobalamin was supplied by Sigma. H_2OCbl was from Roussel. The CN-13-epiCbl was prepared as described in the literature[19,20,24] by acid-catalyzed epimerization of CNCbl in anhydrous trifluoroacetic acid. CN-13-epiCbl was converted to the alkyl-13-epiCbl's as described previously.[24] These complexes were purified and characterized by UV-visible, ^{1}H, ^{13}C and amide ^{15}N NMR spectroscopy as described previously.[22,31]

Instrumentation and measurements

The pH of the solutions was measured using a Mettler Delta 350 pH meter with a combined glass electrode. It was calibrated with standard buffer solutions at pH 7.0 and 10.0. UV-Vis spectra were recorded on Shimadzu UV-2101 and Hewlett Packard 8452A spectrophotometers.

Analytical HPLC was performed on a 4.6 × 250 mm Beckman C_8 ultrasphere column while semipreparative HPLC was performed on a 10 × 250 mm Beckman C_8 ultrasphere column.[24]

Kinetic measurements were carried out on an Applied Photophysics SX 18MV stopped-flow instrument coupled to an online data acquisition system. At least eight kinetic runs were recorded under all conditions, and the reported rate constants represent the mean values. All kinetic measurements were carried out under pseudo-first order conditions, *i.e.* the nucleophile concentration was at least in ten-fold excess. Measurements under high pressure were carried out using a home-made high pressure stopped-flow instrument.[32] Kinetic traces were analysed with the OLIS KINFIT program (Bogart, GA, USA).

The UV-Vis spectrophotometers and stopped-flow instruments were thermostated to the desired temperature ± 0.1 °C. Values of $\Delta H^{\neq}$ and $\Delta S^{\neq}$ were calculated from the slopes and intercepts, respectively, of plots of $\ln(k/T)$ *vs.* $1/T$, and values of $\Delta V^{\neq}$ were calculated from the slope of plots of $\ln(k)$ *vs.* pressure.

Results and discussion

Preliminary experiments at pH 11.0, in which the UV-Vis spectrum was scanned in the range of 300 to 700 nm, showed that CN^- reacts rapidly with the X-13-epiCbl complexes and that the equilibria are established within the mixing and measurement time. The reactions investigated in the present study can be summarized by reaction (1), in which the displacement of DMBz by cyanide (K_{CN1}) to give X(CN)-13-epiCbl occurs.
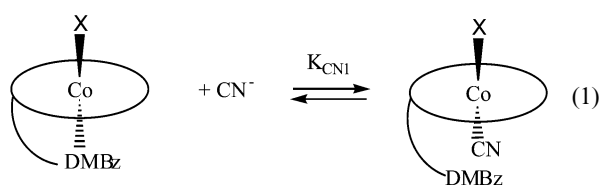
In a preliminary study we first attempted to follow the kinetics of the reaction of Me-13-epiCbl with CN^- at pH 11.0 (Caps buffer) and 5.0 °C. This reaction was found to be too fast to be followed on the stopped-flow instrument (deadtime of ca. 2–4 ms). The product of the reaction, Me(CN)-13-epiCbl, shows a slight increase in absorbance in the range 580–600 nm

and is stable in the dark. We previously reported that the reactions of XCbl with CN^- to form $X(CN)Cbl^-$, where X = Me, CH_2Br, Pr, Et and Ado, are also too fast to be monitored by stopped-flow techniques.[25,26]

Kinetics of the reaction of β-NCCH₂-13-epiCbl with cyanide

Characteristic spectral changes are observed for the reaction of β-NCCH₂-13epi-Cbl with cyanide (see ESI,† Fig. S1). The product spectrum suggests the formation of the intermediate complex, NCCH₂(CN)-13-epiCbl, since new bands appeared at 383, 568 and 606 nm (sh), and this complex is light sensitive, but indefinitely stable in the dark. Fig. 1 shows a plot of k_{obs} *vs.* $[CN^-]$ for the reaction of 4×10^{-5} M β-NCCH₂-13-epiCbl with excess CN^- ($[CN^-]$ = 0.025–1.0 M) at pH 11.0, I = 1.0 M ($NaClO_4$) and 5.0 °C. This plot shows that the observed rate constant decreases on increasing the $[CN^-]$ and then reaches a limiting value of k_{obs} at high $[CN^-]$, which equals k_1 in reaction (2) according to the rate law (derived under steady state conditions for the intermediate species) given in (3), indicating that

$$k_{obs} = \frac{k_1 k_2 [CN^-] + k_{-1} k_{-2}}{k_{-1} + k_2 [CN^-]} \qquad (3)$$

$k_{-2} > k_1$ under such conditions. Interesting to note is that in the case of NCCH₂Cbl, the reverse was found, *viz.* $k_1 \gg k_{-2}$.[26] The intercept of the plot can be assigned to a contribution of the back reaction, whereas the observed curvature can be considered as evidence in favor of a limiting D mechanism as outlined in eqn. (2). The kinetic data are for the substitution reaction that involves displacement of α-DMBz by CN^- as shown in reaction (1).
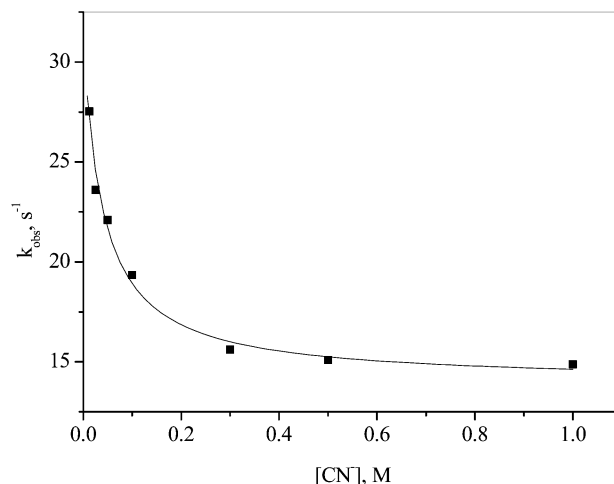

Fig. 1 Plot of k_{obs} *vs.* $[CN^-]$ for the reaction between β-NCCH₂-13-epiCbl and CN^- at pH 11.0, 5.0 °C and I = 1.0 M ($NaClO_4$); the solid line is a fit to eqn. (3) in the text.

On the basis of all the available data, the suggested mechanism for the reaction between β-NCCH2-13-epiCbl and CN^- can be represented by reaction (2), which involves dechelation of DMBz to form a six-coordinate aqua intermediate. The data in Fig. 1 were fitted to eqn. (3) and resulted in k_1 = 14.0 ± 0.6 s^{-1}, k_{-2} = 32 ± 2 s^{-1} and k_2/k_{-1} = 25 ± 7 M^{-1} at 5.0 °C, from which an overall equilibrium constant, $K_{CN} = k_1 k_2 / k_{-1} k_{-2} = 11 \pm$

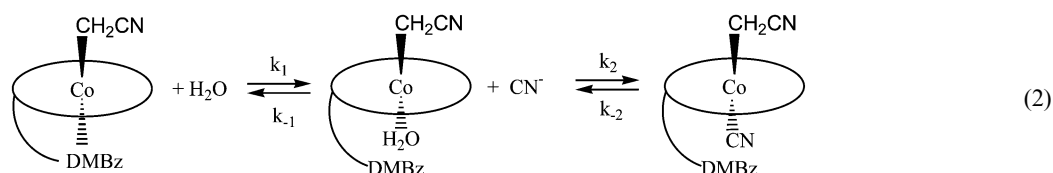**Table 1** Kinetic data for the reaction of (X)-13-epiCbl with CN^- as a function of temperature[a]

	k_{obs}[b]$/s^{-1}$	
$T/°C$	X = CN	X = NCCH_2
5.0		14.9 ± 0.4
10.0		30 ± 1
15.0	0.00203 ± 0.0002	56 ± 4
20.0	0.00404 ± 0.0002	100 ± 6
25.0	0.0090 ± 0.0005	180 ± 13
30.0	0.01845 ± 0.0001	
35.0	0.0368 ± 0.0007	
40.0	0.0725 ± 0.0007	
$\Delta H^{\neq}/kJ\,mol^{-1}$	106 ± 1	83 ± 1
$\Delta S^{\neq}/J\,K^{-1}\,mol^{-1}$	$+82 \pm 4$	$+77 \pm 4$

[a] Experimental conditions: for X = NCCH_2: [NCCH_2-13-epiCbl] = 4×10^{-5} M, $[CN^-]$ = 1.0 M, pH 11.0, I = 1.0 M (NaClO_4). For X = CN: [CN-13-epiCbl] = 5×10^{-5} M, $[CN^-]$ = 0.25 M, pH 11.0, I = 0.5 M (NaClO_4). [b] Under the selected experimental conditions, $k_{obs} = k_1$

2 M^{-1} can be calculated. This value is in a very good agreement with the spectrophotometrically determined value of 13.3 ± 1.5 M^{-1} reported below, but is significantly smaller than that reported for NCCH_2Cbl, *viz.* 63.8 M^{-1}.[33] This difference shows that the affinity of CN^- for cobalamin is *ca.* 6 times higher than for 13-epicobalamin. The value of k_1 for the reaction of NCCH_2Cbl with CN^- (64.7 s^{-1})[26] is significantly higher than that obtained here for NCCH_2-13-epiCbl (*viz.* 14.0 s^{-1}). The value of k_2/k_{-1}, which represents the efficiency of cyanide compared to DMBz of the nucleotide loop to scavenge the six-coordinate intermediate, was found to be 25 M^{-1} for of NCCH_2-13-epiCbl, which is very similar to that of NCCH_2Cbl (*viz.* 27.9 M^{-1}).[26] The difference between k_1 for NCCH_2Cbl and NCCH_2-13-epiCbl can indeed be ascribed to the presence or absence of the *e*-side chain on the α face, which decreases k_1 in the case of 13-epicobalamin and consequently also decreases the overall equilibrium constant. This suggests that in the normal Cbl, the presence of a "downward" projecting propionamide side chain at C13 sterically destabilizes the base-on species.

The reaction between β-NCCH_2-13-epiCbl and CN^- was studied as a function of temperature and pressure at a high cyanide concentration (1.0 M), *i.e.* where $k_{obs} = k_1$, and the results are reported in Table 1 and Fig. 2(a), respectively. Fig. 2(a) demonstrates a good linear correlation between $\ln(k)$ and pressure. The activation parameters $\Delta H^{\neq}$ and $\Delta S^{\neq}$ were found to be 83 ± 1 $kJ\,mol^{-1}$ and $+77 \pm 4$ $J\,K^{-1}\,mol^{-1}$, respectively, and the activation volume, $\Delta V^{\neq} = +13.3 \pm 1.0$ $cm^3\,mol^{-1}$ at 0.0 °C. These data, along with the observed rate law and saturation kinetics for cyanide substitution, suggest that the first step of the reaction of β-NCCH_2-13-epiCbl with CN^- (k_1) indeed follows a limiting D mechanism, *i.e.* a dissociative dechelation of DMBz followed by coordination of water to the vacant coordination site. It was found previously that $\Delta H^{\neq}$, $\Delta S^{\neq}$ and $\Delta V^{\neq}$ for the reaction of NCCH_2Cbl with CN^- are 85 ± 2 kJ mol^{-1}, $+97 \pm 6$ $J\,K^{-1}\,mol^{-1}$ and $+12.7 \pm 0.5$ $cm^3\,mol^{-1}$, respectively.[26] It seems clear that these data are indeed comparable, suggesting that a limiting D mechanism is operating in both cases. We have also recently reported values for $\Delta V^{\neq}$ of +13.1 and +14.8 $cm^3\,mol^{-1}$ for the reactions of CNCbl and β-CF_3Cbl with CN^-.[25,26] Furthermore, the volume of activation for the reaction of β-(*N*-methylimidazolyl)cobalamin with N-methylimidazole was also reported to be significantly positive, *viz.* $+15.0 \pm 0.7$ and $+16.8 \pm 1.1$ $cm^3\,mol^{-1}$ at 5×10^{-3} and 1 M N-methylimidazole, respectively, which correspond to the aquation of (N–MeIm)_2Cbl^+ and the dechelation reaction of the α-DMBz of (N–MeIm)Cbl^+, respectively.[34] These $\Delta V^{\neq}$ values are typical of those expected for a limiting D substitution mechanism for an octahedral complex.[35,36]
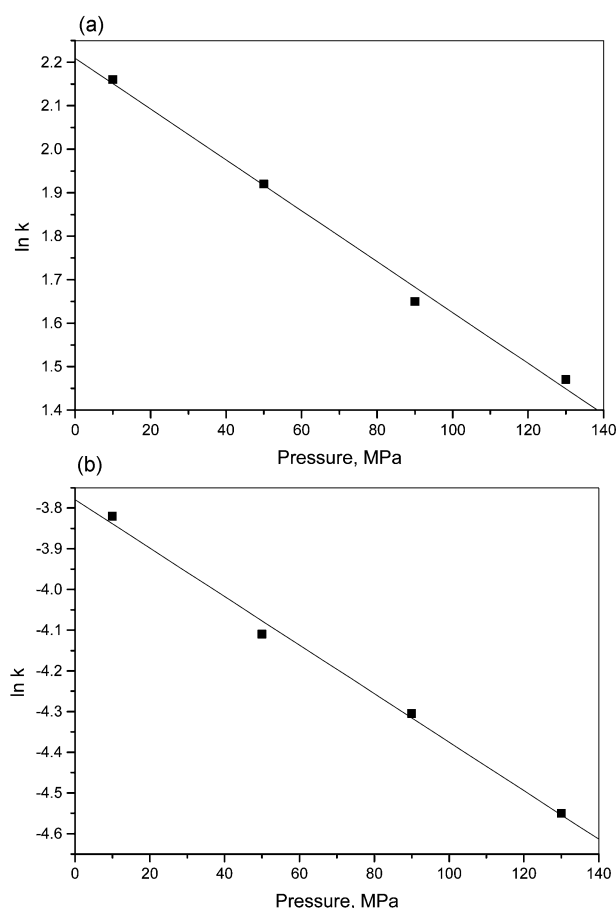

Fig. 2 (a) Plot of $\ln k_{obs}$ *vs.* pressure for the reaction between β-NCCH_2-13-epiCbl and CN^- measured at 1.0 M CN^-; the best fit of the data (solid line) gives $\Delta V^{\neq} = +13.3 \pm 1.0$ at 0.0 °C. (b) Plot of $\ln k_{obs}$ *vs.* pressure for the reaction between β-CN-13-epiCbl and CN^- measured at 0.25 M CN^-; the best fit of the data (solid line) gives $\Delta V^{\neq} = +14.8 \pm 1.2$ $cm^3\,mol^{-1}$ at 30.0 °C.
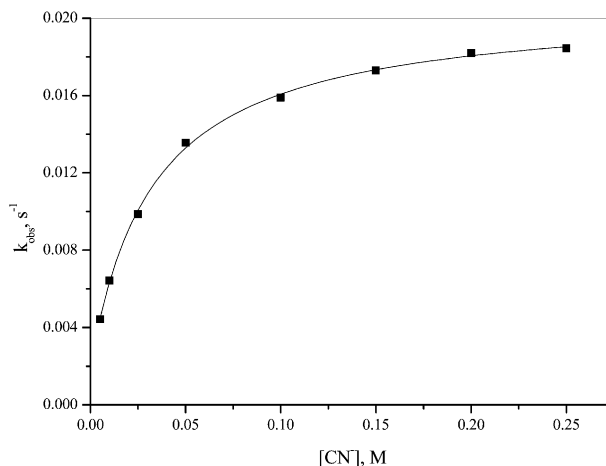

Fig. 3 Plot of k_{obs} *vs.* $[CN^-]$ for the reaction between CN-13-epiCbl and CN^- at pH 11.0, 30.0 °C and I = 0.5 M (NaClO_4); the solid line is a fit to eqn. (3) in the text.

Kinetics of the reaction of CN-13-epiCbl with CN^-

Fig. 3 shows a plot of k_{obs} *vs.* $[CN^-]$ for the reaction of 5×10^{-5} M CN-13-epiCbl with excess CN^- ($[CN^-]$ = 0.01 to 0.25 M) at pH 11.0, I = 0.5 M (NaClO_4) and 30.0 °C. This plot also shows saturation kinetics at high cyanide concentrations but in the opposite direction from the NCCH_2-13-epiCbl case reported above. A limiting value of k_{obs} is reached at high $[CN^-]$, and the intercept and observed curvature can be interpreted in the same way as before. The reported kinetic data are for the substitution

of α-DMBz by CN^-, since new bands were observed at 367, 540 (sh) and 580 nm, characteristic for $(CN)_2$-13-epiCbl.

The data in Fig. 3 were fitted to eqn. (3) and resulted in $k_1 = 0.0207 \pm 0.0002$ s^{-1}, $k_{-2} = (2.0 \pm 0.3) \times 10^{-3}$ s^{-1} and $k_2/k_{-1} = 31 \pm 2$ M^{-1} at 25.0 °C, from which an overall equilibrium constant $K_{CN} = k_1k_2/k_{-1}k_{-2} = 320 \pm 60$ M^{-1} was calculated. This value is in a good agreement with the spectrophotometrically determined value of 350 ± 21 M^{-1} reported below. Interestingly, in this case, $k_1 \gg k_{-2}$, which accounts for the opposite trend in the cyanide concentration dependence of k_{obs} (compare Figs. 1 and 3) and is similar to that reported previously in the case of CNCbl.[26] The limiting rate constant value k_1 (0.0207 s^{-1}) is smaller than that obtained in the case of CNCbl (0.042 s^{-1}).[26,37] However, the value of k_2/k_{-1} (31 ± 2 M^{-1}), which represents the efficiency of cyanide compared to DMBz of the nucleotide loop to scavenge the six-coordinate intermediate, was found to be similar to that obtained previously in the case of CNCbl (36.9 M^{-1}).[26]

The reaction between CN-13-epiCbl and CN^- was studied as a function of temperature and pressure at a high cyanide concentration (0.25 M), i.e. where $k_{obs} = k_1$, and the results are reported in Table 1 and Fig. 2(b), respectively. Fig. 2(b) demonstrates a good linear correlation between $\ln(k)$ and pressure. The activation parameters $\Delta H^{\neq}$ and $\Delta S^{\neq}$ were found to be 106 ± 1 kJ mol^{-1} and $+82 \pm 4$ J K^{-1} mol^{-1}, respectively, and the activation volume, $\Delta V^{\neq} = +14.8 \pm 1.2$ cm^3 mol^{-1} at 30.0 °C. These data along with the observed rate law suggest that the reaction of CN-13-epiCbl with CN^- also follows a limiting D mechanism involving dissociative dechelation of DMBz to form a six-coordinate intermediate aqua complex. This mechanism is in agreement with our suggestion for the reactions of $NCCH_2$-13-epiCbl and XCbl (X = CN^-, CF_3, $NCCH_2$)[25,26] with CN^- and that suggested by Reenstra and Jencks,[37] where they also found that the rate of CN^- addition to CNCbl reaches a limiting value at high $[CN^-]$.

Kinetics of the base-on/base-off equilibration

We[27] have recently shown that evidence for the suggested dissociative mechanism for the reaction of XCbl with CN^- could be obtained from the direct measurement of the dechelation rate constant of DMBz (k_1) through acidification of XCbl to produce the protonated base-off species. However, in the present study (X-13-epiCbl), $pK_{base-off}$ values are less than those reported for XCbl, viz. $pK_{base-off}$ for CN-13-epiCbl and $NCCH_2$-13-epiCbl were found to be -0.9 and 0.85, respectively.[24] These low values require a very high acid concentration to dechelate DMBz in the α-position. On the other hand, the DMBz dissociation rate of $NCCH_2$-13-epiCbl and CN-13-epiCbl can be followed with the stopped flow technique, since, from the electron inductive effect of these substituents, the rate of DMBz dissociation is expected to be slower for these complexes than for those with strongly donating X substituents. The DMBz dissociation rate of other X-13-epiCbl's, such as Me-13-epiCbl and Et-13-epiCbl, are much too fast to be monitored by stopped-flow techniques.

Kinetic results for the stopped-flow "pH-jump" reaction of 6×10^{-5} M β-$NCCH_2$-13-epiCbl (pH 5, unbuffered solution) with different concentrations of $HClO_4$ (0.01–1.0 M) at $I = 2$ M ($NaClO_4$) and 5.0 °C are shown in Fig. 4. The values of k_{obs} first decrease with increasing acid concentration in the lower concentration range (0.005–0.05 M), and then gradually increase linearly with increasing acid concentration (0.05–0.3 M). A combination of these concentration dependencies results in the curved dependence observed in Fig. 4. The first part of the plot at low acid concentration is incomplete since it was not possible to follow the reaction at lower acid concentrations where it becomes too fast to be followed by stopped-flow and the change in absorbance becomes too small. The second part of the plot is expected to level off to reach k_1, but shows an increase in k_{obs}
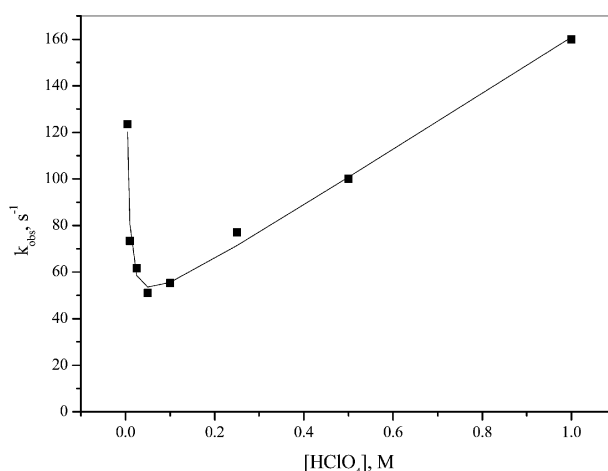

Fig. 4 Plot of k_{obs} vs. $[HClO_4]$ for the reaction between β-$NCCH_2$-13epiCbl and $HClO_4$ at 5.0 °C and $I = 2$ M ($NaClO_4$); the solid line is a fit to eqn. (4) in the text.

with increasing acid concentration. This linear increase in k_{obs} is ascribed to an acid-catalyzed dechelation reaction, the slope of which represents the rate constant for the acid-catalyzed process (k^H) and the intercept of which represents the rate constant for the spontaneous dechelation of DMBz (viz. k_1). The increase in k_{obs} with increasing acid concentration was in this case not as prominent as in the case of XCbl,[27] because the value of $pK_{base-off}$ in the present case is only 0.85,[24] which means that more acidic conditions are required to reach significant concentrations of the protonated base-off cobalamin. It is reasonable to conclude that dechelation of DMBz to give β-$NCCH_2$-13-epiCbl (base-off) is catalyzed by acid, in agreement with recently reported data for the dechelation of DMBz in a series of XCbl's.[27]

In terms of the overall base-on/base-off equilibration for the spontaneous and acid-catalyzed pathways discussed in detail before,[27] the rate law for the acidification reaction of β-$NCCH_2$-13-epiCbl is given in eqn. (4), in which k_1 and k_{-1} represent the rate constants for the spontaneous dechelation and chelation of X-13-epiCbl in reaction (2), respectively, k^H represents the acid-catalysed reaction path, and K_{Bz} represents the acid-dissociation constant for the dechelated $DMBzH^+$ species.

$$k_{obs} = k_1 + \frac{k_{-1}K_{Bz}}{K_{Bz} + [H^+]} + k^H[H^+] \qquad (4)$$

A non-linear least squares fit of the data shown in Fig. 4 to the rate law in (4) using $pK_{Bz} = 5.56$,[38] results in $k_1 = 39 \pm 3$ s^{-1}, $k_{-1} = (1.5 \pm 0.1) \times 10^5$ s^{-1} and $k^H = 121 \pm 7$ M^{-1} s^{-1}. It follows that K_{Co} (= k_{-1}/k_1) equals 3700, which is less than the value previously reported from thermodynamic considerations (viz. 5.1×10^4).[24] The value of k_2/k_{-1} calculated from the linear fit of the experimental data obtained from the cyanide concentration dependence (see above) to eqn. (3) was found to be 25 M^{-1}. Combined with the value of k_{-1} (1.5×10^5 s^{-1}), the value of k_2 can be calculated to be 3.75×10^6 M^{-1} s^{-1}. The value of k_1 is not in good agreement with the acid-independent limiting rate constant (14.0 s^{-1}) obtained when the nucleophile concentration dependence was studied for the reaction of β-$NCCH_2$-13-epiCbl and CN^- (see above). The likely reason for the inconsistency of the results is the low value of $pK_{base-off}$ which requires a very high concentration of $HClO_4$. In addition, the H^+-catalyzed contribution to the observed rate constant is already greater than the uncatalyzed rate at $[HClO_4] = 0.5$ M, such that the limiting value of k_1 cannot be reached.

Similar results were obtained for the reaction of CN-13-epiCbl with $HClO_4$. The data for the reaction of 8×10^{-5} M CN-13-epiCbl with $HClO_4$ (0.01–1.0 M) at 30.0 °C are shown in

Table 2 Kinetic, thermodynamic and activation parameter data for the reaction of (X)Cbl and (X)-13-epiCbl with CN^-

		Cbl[a]		13-epiCbl[b]	
X =		$NCCH_2$	CN	$NCCH_2$	CN
$k_1{}^c$/s^{-1}		64.7 ± 0.7	0.042 ± 0.001	14.0 ± 0.6	0.0207 ± 0.0002
$k_{-1}{}^c$/s^{-1}		27.4 ± 0.8	$(7 \pm 3) \times 10^{-5}$	32 ± 2	$(2.0 \pm 0.3) \times 10^{-3}$
$(k_2/k_{-1})^c$/M^{-1}		27.9 ± 2.7	36.9 ± 1.5	25 ± 7	31 ± 2
$K_{CN}{}^d$/M^{-1}		63.8 ± 1.4^e	1×10^{4f}	13.3 ± 1.5	350 ± 21
$\Delta H^{\neq}$/kJ mol^{-1}		85 ± 2	105 ± 2	83 ± 1	106 ± 1
$\Delta S^{\neq}$/J K^{-1} mol^{-1}		$+97 \pm 6$	$+81 \pm 6$	$+77 \pm 4$	$+82 \pm 4$
$\Delta V^{\neq}$/cm^3 mol^{-1}		$+12.7 \pm 0.5$	$+13.1 \pm 0.3$	$+13.3 \pm 1.0$	$+14.8 \pm 1.2$

[a] Data from ref. 26 unless otherwise stated. [b] This work. [c] Calculated from a non-linear fit of the experimental data to eqn. (3) in the text. [d] Determined by spectrophotometric method. [e] Ref. 33. [f] Ref. 37.

the ESI†(Fig. S2). The data again show a decrease in k_{obs} and then level off at high concentration of HClO$_4$, and no sign for an acid catalyzed reaction was observed in this case. This is expected since the p$K_{base-off}$ value in this case is -0.9, which will require a much higher acid concentration for the acid-catalyzed pathway to play a meaningful role.[24] The non-linear least squares fit of the data to the rate-law in eqn. (4) without the $k^H[H^+]$ term, resulted in $k_1 = 0.18 \pm 0.03$ s^{-1} and $k_{-1} = (1.79 \pm 0.06) \times 10^4$ s^{-1}, respectively. It follows that $K_{Co} = 9.9 \times 10^4$, which is less than that reported before, viz. 2.9×10^6.[24] The value of k_2/k_{-1} calculated from the linear fit of the experimental data obtained from the cyanide concentration dependence (see above) to eqn. (3) was found to be 31 M^{-1}. Combined with the value of k_{-1} (1.79×10^4 s^{-1}), it follows that $k_2 = 5.6 \times 10^5$ M^{-1} s^{-1}.

By way of comparison, the value of k_1 for the dechelation and k_{-1} for the chelation reaction of NCCH$_2$-13-epiCbl were found to be 39 and 1.5×10^5 s^{-1}, respectively, whereas those for CN-13-epiCbl were found to be 0.18 and 1.79×10^4 s^{-1}, respectively. These rate constants nicely show the effect of the axial group (X) in the upper β-position on the substitution rate constant of DMBz located in the α-position, trans to X, by CN$^-$.

Equilibrium measurements

The spectrophotometric titration of β-NCCH$_2$-13-epiCbl with CN$^-$ was monitored by following the increase in absorbance at 600 nm, where the largest change in absorbance occurred. Selected data are shown in Fig. 5, where the solid line represents a fit of the data to eqn. (5).

$$A_x = A_0 + (A_\infty - A_0)K_{CN1}[CN^-]/(1 + K_{CN1}[CN^-]) \quad (5)$$

The values of A_0 and A_∞ represent the absorbances of β-NCCH$_2$-13-epiCbl and (β-NCCH$_2$)(α-CN)-13-epiCbl, respec-
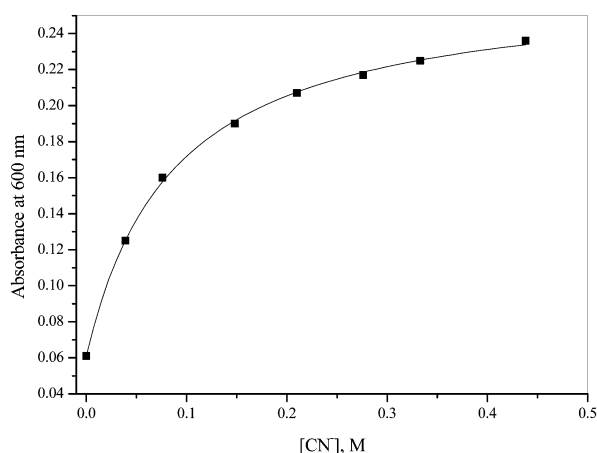

Fig. 5 Change in absorbance at 600 nm on addition of CN$^-$ to NCCH$_2$-13-epiCbl; the solid line is a fit to eqn. (5) in the text and results in $K_{CN1} = 13.3 \pm 1.5$ M^{-1}.

tively, and A_x is the absorbance at any cyanide concentration. The values of K_{CN1} and A_∞ were calculated from eqn. (5), and K_{CN1} was found to be 13.3 ± 1.5 M^{-1}. This value is in a good agreement with that determined kinetically (11 ± 2 M^{-1}). The analysis of these data by plotting log $(A_x - A_0)/(A_\infty - A_x)$ vs. log[CN$^-$] gave a good linear plot with a slope of 1.09 ± 0.05, which indicates one CN$^-$ ligand is coordinated to the cobalt atom.

A similar spectrophotometric titration was carried out for CN-13-epiCbl with CN$^-$ and the spectral changes that accompany this titration are shown in Fig. 6. The spectrophotometric titration was monitored by following the increase in absorbance at 580 nm, where the largest change in absorbance occurred, and selected data are shown in the ESI†(Fig. S3). The value of K_{CN1} in this case was found to be 350 ± 21 M^{-1}. This value is in a good agreement with that determined kinetically (viz. 320 M^{-1}).
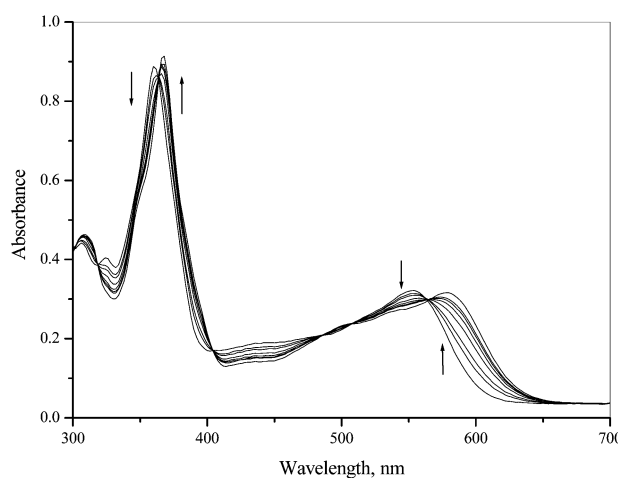

Fig. 6 UV-Vis spectra of CN-13-epiCbl recorded in the presence of various concentrations of CN$^-$ (5×10^{-4}–0.011 M) at pH 11.0, $I = 0.5$ and at 30.0 °C.

Overall discussion

Table 2 summarizes the kinetic, thermodynamic and activation parameter data obtained for the reaction of XCbl and X-13-epiCbl with CN$^-$. It is clear from this table that the values of K_{CN} for the reactions of NCCH$_2$-13-epiCbl and CN-13-epiCbl with CN$^-$ (13.3 and 350 M^{-1}, respectively) are smaller than those obtained for the same reactions of NCCH$_2$Cbl and CNCbl with cyanide (63.8 and 10^4 M^{-1}, respectively).[33,37] Table 2 also shows the significant decrease in the rate constant, k_1, for 13-epicobalamins compared to the cobalamins. These differences are ascribed to the epimerization of the e side chain from a "downward" axial position to an "upward" axial position, which makes the displacement of DMBz (α-position) by CN$^-$ slower in the case of the 13-epicobalamins and the overall equilibrium constant smaller. It is already known that epimerization

at C13 causes a decrease in the $pK_{base\text{-}off}$ value of about 0.83 ± 0.14 across the series of XCbl's and a corresponding increase in K_{Co} for a given X. K_{Co} was found to be 6.9 ± 1.8 fold higher for the X-13-epiCbl's than for the XCbl's.[24]

In terms of the substitution lability of the X-13-epiCbl's, the results of this study have shown that epimerization at C13 has a sensitive influence on the relative magnitudes of the rate constants in the reaction sequence (2), which through rate law (3) can have a remarkable influence on the observed dependence of the pseudo first order substitution rate constant on the entering nucleophile concentration as demonstrated by the results in Figs. 1 and 3, and summarized in Table 2. This is caused by the relative size of k_1 and k_{-2}, which controls the rate of the ligand dissociation steps in the forward and reverse directions, and is very sensitive to epimerization at C13.

Structural studies on the ground state *trans* effect suggest that epimerization at C13 does not affect the Co–C bond enthalpies, and would therefore be unlikely to affect the enthalpies of activation for Co–C bond cleavage but tend to increase the activation entropies.[39] The values of $\Delta H^{\neq}$, $\Delta S^{\neq}$ and $\Delta V^{\neq}$ for the reaction of X-13-epiCbl with CN^- are included in Table 2. The values for $\Delta S^{\neq}$ and $\Delta V^{\neq}$ show the same mechanistic trends and support the suggested dissociative mechanism. The substitution reactions of β-NCCH2-13-epiCbl and β-CN-13-epiCbl with CN^- involve rate-determining displacement of α-DMBz that proceeds through a limiting D mechanism.

This study has revealed how the alkyl ligands in XCbl and X-13-epiCbl control the kinetics and thermodynamics of the reaction with CN^-, and how epimerization at C-13 decreases the rate constant for the axial ligand substitution reaction, but does not affect the mechanism of the substitution process.

Acknowledgements

References

1 C. L. Drennan, S. Huang, J. T. Drummond, R. G. Matthews and M. L. Ludwig, *Science*, 1994, **266**, 1669.

2 C. L. Drennan, R. G. Matthews and M. L. Ludwig, *Curr. Opin. Struct. Biol.*, 1994, **4**, 919.

3 B. T. Golding and W. Buckel, *in Comprehensive Biological Catalysis*, ed. M. L., Sinnott, Academic Press, London, 1997, vol. III, pp. 239–259.

4 F. Mancia, N. H. Keep, A. Nakagawa, P. F. Leadlay, S. McSweeney, B. Ramussen, P. Boscke, O. Diat and P. R. Evans, *Structure*, 1996, **4**, 229.

5 R. Reiter, G. Gruber, G. Jogl, V. G. Wagner, H. Bothe, V. Buckel and C. Kratky, *Structure*, 1999, **7**, 891.

6 C. H. Chang and P. A. Frey, *J. Biol. Chem.*, 2000, **275**, 106.

7 K. L. Brown, X. Zou and L. Salmon, *Inorg. Chem.*, 1991, **30**, 1949.

8 Y. W. Alelyunas, P. E. Fleming, R. G. Finke, T. G. Pagano and L. G. Marzilli, *J. Am. Chem. Soc.*, 1991, **113**, 3781.

9 K. L. Brown and X. Zou, *J. Am. Chem. Soc.*, 1992, **114**, 9643.

10 X. Zou, K. L. Brown and C. Vaughn, *Inorg. Chem.*, 1992, **31**, 1552.

11 K. L. Brown and X. Zou, *Inorg. Chem.*, 1992, **31**, 2541.

12 K. L. Brown, L. Salmon and J. A. Kirby, *Organometallics*, 1992, **11**, 422.

13 X. Zou and K. L. Brown, *J. Am. Chem. Soc.*, 1993, **115**, 6689.

14 H. M. Marques, L. Knapton, X. Zou and K. L. Brown, *J. Chem. Soc., Dalton Trans.*, 2002, 3195.

15 (*a*) M. I. Yakusheva, A. A. Pozanskaya, T. A. Pospeiova, I. P. Rudakova, A. M. Yurkevich and V. A. Yakovlev, *Biochim. Biophys. Acta.*, 1977, **484**, 216; (*b*) T. Toraya, E. Krodel, A. S. Mildvan and R. H. Abeles, *Biochemistry*, 1979, **189**, 417; (*c*) C. G. D. Morley, R. L. Bakley and H. P. C. Hogenkamp, *Biochemistry*, 1968, **7**, 1231; (*d*) D. L. Anton, P. K. Tsai and H. P. C. Hogenkamp, *J. Biol. Chem.*, 1980, **255**, 4507; (*e*) T. Toraya and S. Fukui, *Adv. Chem. Ser.*, 1980, **191**, 139.

16 (*a*) T. Tamao, Y. Morikawa, S. Shimizu and S. Fukui, *Biochim. Biophys. Acta.*, 1968, **151**, 260; (*b*) T. Toraya, T. Shirakashi, S. Fukui and H. P. C. Hogenkamp, *Biochemistry*, 1975, **14**, 3949.

17 (*a*) T. Toraya and A. Ishida, *J. Biol. Chem.*, 1991, **266**, 5430; (*b*) T. Toraya, S. Miyoshi, M. Mori and K. Wada, *Biochim. Biophys. Acta.*, 1994, **1204**, 169.

18 (*a*) G. N. Sando, R. L. Blakley, H. P. C. Hogenkamp and P. J. Hoffman, *J. Biol. Chem.*, 1975, **250**, 8774; (*b*) K. Ushio, S. Fukui and T. Toraya, *Biochim. Biophys. Acta*, 1984, **788**, 318; (*c*) T. Toraya, T. Matsumoto, M. Ichikawa, T. Itoh, T. Sugawara and Y. Mizuno, *J. Biol. Chem.*, 1986, **261**, 9289.

19 R. Bonnett, J. M. Godfrey, V. B. Math, E. Edmond, H. Evans and O. J. R. Hodder, *Nature*, 1971, **229**, 473.

20 R. Bonnett, J. M. Godfrey and V. B. Math, *J. Chem. Soc. C*, 1971, 3736.

21 H. Stoeckli-Evans, E. Edmond and D. C. Hodgkin, *J. Chem. Soc., Perkin Trans. 2*, 1972, 605.

22 K. L. Brown, D. R. Evans, J. D. Zubkoswski and E. J. Valente, *Inorg. Chem.*, 1996, **35**, 415.

23 H. M. Marques and K. L. Brown, *J. Mol. Struct. (THEOCHEM)*, 1995, **340**, 97.

24 K. L. Brown and G.-Z. Wu, *Inorg. Chem.*, 1994, **33**, 4122.

25 M. S. A. Hamza, X. Zou, K. L. Brown and R. van Eldik, *Inorg. Chem.*, 2001, **40**, 5440.

26 M. S. A. Hamza, X. Zou, K. L. Brown and R. van Eldik, *J. Chem. Soc., Dalton Trans.*, 2002, 3832.

27 M. S. A. Hamza, X. Zou, K. L. Brown and R. van Eldik, *Eur. J. Inorg. Chem.*, 2003, 268.

28 N. E. Brasch, M. S. A. Hamza and R. van Eldik, *Inorg. Chem.*, 1997, **36**, 3216.

29 M. S. A. Hamza, A. G. Cregan, N. E. Brasch and R. van Eldik, *Dalton Trans.*, 2003, 596.

30 *Chemistry and Biochemistry of B_{12}*, ed. R. Banerjee, Wiley & Sons Inc.New York, 1999.

31 K. L. Brown, H. B. Brooks, B. D. Gupta, M. Victor, H. M. Marques, D. C. Scooby, W. J. Goux and R. Timkovich, *Inorg. Chem.*, 1991, **30**, 3430.

32 R. van Eldik, W. Gaede, S. Wieland, T. Kraft, M. Spitzer and D. M. Palmer, *Rev. Sci. Instrum.*, 1993, **64**, 1355.

33 K. L. Brown, *J. Am. Chem. Soc.*, 1987, **109**, 2277.

34 A. G. Cregan, N. E. Brasch and R. van Eldik, *Inorg. Chem.*, 2001, **40**, 1430.

35 T. W. Swaddle, *Rev. Phys. Chem. Jpn.*, 1980, **50**, 230.

36 (*a*) R. van Eldik, T. Asano and W. J. Le Noble, *Chem. Rev.*, 1989, **89**, 549; (*b*) A. Drljaca, C. D. Hubbard, R. van Eldik, T. Asano, M. V. Basilevsky and W. J. Le Noble, *Chem. Rev.*, 1998, **98**, 2167.

37 W. W. Reenstra and W. P. Jencks, *J. Am. Chem. Soc.*, 1979, **101**, 5780.

38 K. L. Brown, J. M. Hakimi, D. M. Nuss, Y. D. Montejano and D. W. Jacobsen, *Inorg. Chem.*, 1984, **23**, 1463.

39 K. L. Brown, X. Zou and D. R. Evans, *Inorg. Chem.*, 1994, **33**, 5713.